
SE3Set: Harnessing equivariant hypergraph neural networks for molecular representation learning

Hongfei Wu*

College of Chemistry and Molecular Engineering,
Peking University, Beijing, 100871, China

Lijun Wu

Microsoft Research AI4Science,
Beijing, 100084, China

Guoqing Liu

Microsoft Research AI4Science,
Beijing, 100084, China

Zhirong Liu

College of Chemistry and Molecular Engineering,
Peking University, Beijing, 100871, China
LiuZhiRong@pku.edu.cn

Bin Shao

Microsoft Research AI4Science,
Beijing, 100084, China
binshao@microsoft.com

Zun Wang

Microsoft Research AI4Science,
Beijing, 100084, China
zunwang@microsoft.com

Abstract

In this paper, we develop SE3Set, an SE(3) equivariant hypergraph neural network architecture tailored for advanced molecular representation learning. Hypergraphs are not merely an extension of traditional graphs; they are pivotal for modeling high-order relationships, a capability that conventional equivariant graph-based methods lack due to their inherent limitations in representing intricate many-body interactions. To achieve this, we first construct hypergraphs via proposing a new fragmentation method that considers both chemical and three-dimensional spatial information of molecular system. We then design SE3Set, which incorporates equivariance into the hypergraph neural network. This ensures that the learned molecular representations are invariant to spatial transformations, thereby providing robustness essential for accurate prediction of molecular properties. SE3Set has shown performance on par with state-of-the-art (SOTA) models for small molecule datasets like QM9 and MD17. It excels on the MD22 dataset, achieving a notable improvement of approximately 20% in accuracy across all molecules, which highlights the prevalence of complex many-body interactions in larger molecules. This exceptional performance of SE3Set across diverse molecular structures underscores its transformative potential in computational chemistry, offering a route to more accurate and physically nuanced modeling.

1 Introduction

Molecular representation [1, 2, 3] is pivotal for cheminformatics [4], impacting the prediction of molecular properties in drug discovery and material science. Traditional descriptors like fingerprints capture basic structural and energetic aspects of molecules by considering mainly one- and two-body interactions. However, they often miss complex electronic correlations and collective behaviors important for understanding phenomena such as chemical reactivity and protein folding. To address this, advanced methods that include many-body interactions are crucial for a more comprehensive

*These authors did this work during an internship at Microsoft Research AI4Science.

molecular characterization. These methods enhance the predictive capabilities of computational models by more accurately reflecting the intricate dynamics and properties of molecules, which are essential for a deeper understanding of their functionality and reactivity in cheminformatics.

Graph neural networks (GNNs) [5, 6] a foundational tool for representing structured data in molecular sciences with atoms as nodes and chemical bonds as edges, respectively. GNN models excel in tasks ranging from property prediction to reaction simulation [7, 8, 9]. GNNs can capture higher-order molecular interactions through message passing [10] but face overfitting and inefficiency challenges [11, 12]. Architectural improvements in GNNs facilitate the modeling of complex interactions, overcoming some limitations of deep networks [13, 14, 15]. Advances demonstrate the potential of architectural enhancements in GNNs to represent complex interactions [16, 17, 18, 19, 20, 21], but efficiently integrating many-body interactions into these networks is an ongoing challenge [22].

To address the complexities of many-body interactions in molecular systems, hypergraphs offer a compelling alternative to complex GNN architectures. Hypergraphs, with hyperedges connecting multiple vertices, can naturally represent many-body phenomena like electronic delocalization and collective vibrations. This allows for a more accurate modeling of molecular intricacies beyond the limitations of traditional graphs. Integrating hypergraphs with machine learning, particularly through Hypergraph Neural Networks (HGNNs), is an emerging research area. HGNNs manage the flow of information across hyperedges, capturing complex multi-atom interactions and enriching molecular representations. This technique promises to balance model expressiveness with computational efficiency. By innately encoding many-body interactions, HGNNs stand to significantly advance cheminformatics, offering a new approach to molecular property prediction and simulation that resonates with the actual behavior of chemical systems.

In this work, we introduce SE3Set, an innovative approach that enhances traditional GNNs by exploiting hypergraphs for modeling many-body interactions, while ensuring SE(3) equivariant representations that remain consistent regardless of molecular orientation. Our key contributions are:

- A new fragmentation method for hypergraph construction that seamlessly integrates 2D chemical and 3D spatial information, enriching the molecular structure representation.
- The deployment of hypergraph neural networks to capture many-body interactions, providing a deeper insight into molecular behavior that surpasses conventional pairwise modeling.
- The incorporation of SE(3) equivariance within our hypergraph framework, guaranteeing orientation-independent molecular representations.
- SE3Set underwent a comprehensive benchmarking process, exhibiting comparable outcomes to state-of-the-art (SOTA) models on small molecule datasets QM9 and MD17. It demonstrated exceptional performance on the larger molecule dataset MD22, where higher-order interactions are more evident, surpassing SOTA models with a significant reduction in mean absolute errors (MAEs) by an average of roughly 20%. This confirms SE3Set’s efficacy in capturing the complexity of molecular representations.

These advances establish SE3Set as a formidable tool for molecular representation learning, with implications for computational chemistry and beyond.

2 Related works

2.1 Graph neural networks

Message passing neural networks (MPNNs), a class of graph neural networks, are essential for learning node features by transmitting information along graph edges, a process crucial for interpreting structured data like molecules [10]. Equivariant GNNs are especially important for molecular modeling. They adopt either group representation methods, aligning architectures to symmetry groups for improved interaction modeling [23, 24, 25, 15, 26, 27, 20], or direction-based methods that incorporate spatial information for accurate molecular representations [28, 29, 30, 13, 16, 14, 18, 17, 31, 21] and have been engineered to handle intricate up to five-body interactions [22].

2.2 Hypergraph neural networks

Hypergraph Neural Networks (HGNNs) enhance GNNs by incorporating multi-node hyperedges, better capturing complexity in data from various domains. They advance GNNs’ binary interactions with methods like clique expansion for compatibility with existing algorithms [32, 33] and employ tensor techniques for improved hypergraph-based feature learning [34, 35, 36, 37, 38]. While equivariant HGNNs adeptly handle node permutations, preserving data symmetries [39, 40], they often miss 3D spatial transformations, crucial for physical system modeling. In computational chemistry, hypergraph algorithms simulate complex behaviors and optimize molecules through hypergraph grammar [41, 42, 43], providing multidimensional insights into molecular structures [44, 45, 46]. Despite their promise, these methods still face hurdles in integrating spatial information effectively.

2.3 Fragmentation methods

Fragmentation methods break down complex molecules for simpler *ab initio* QM computations of properties, later combining these for a holistic view [47, 48]. Leveraging the localized nature of chemical reactions, these techniques aim for scalable algorithms suitable for large molecule analysis. While instrumental in computational pretraining [49, 50, 51], they typically neglect the fusion of 2D structural with 3D spatial data. Hence, we advocate for a refined fragmentation approach that merges chemical properties with spatial context, potentially advancing hypergraph-based chemical modeling.

3 Preliminaries

3.1 Equivariance

Consider a function \mathcal{L} that maps inputs from space \mathcal{X} to outputs in space \mathcal{Y} . \mathcal{L} is called G -equivariant if it preserves the symmetry of a group G across mappings, meaning for each $g \in G$, we have:

$$\mathcal{L} \circ D^{\mathcal{X}}(g) = D^{\mathcal{Y}}(g) \circ \mathcal{L}, \tag{1}$$

where $D^{\mathcal{X}}$ represents the group G ’s action on \mathcal{X} . This ensures that the function \mathcal{L} reflects changes made to inputs by G in its outputs.

3.2 Hypergraph

Hypergraphs elegantly capture the essence of higher-order interactions among multiple entities, making them an invaluable tool for representing complex relational data. Let $\mathcal{G} = (V, E)$ be a hypergraph with N vertices and M hyperedges, where V represents a set of nodes and E is a set of hyperedges. Distinguishing itself from a traditional graph, a hyperedge can encompass multiple nodes, not limited to two, i.e. each hyperedge $e \in E$ is a non-empty subset of V .

3.3 AllSet

The AllSet framework [52], an advanced HGNN model, addresses heuristic propagation rule limitations in HGNNs by integrating Deep Sets [53] and Set Transformers [54] principles. It uses task-optimized dual multiset functions that maintain permutation invariance, crucial for hypergraph learning. The update rules in AllSet are:

$$Z_{e,:}^{(t+1),v} = f_{\mathcal{V} \rightarrow \mathcal{E}}(V_{e \setminus v, X^{(t)}}; Z_{e,:}^{(t),v}, X_{v,:}^{(t)}), \tag{2}$$

$$X_{v,:}^{(t+1)} = f_{\mathcal{E} \rightarrow \mathcal{V}}(E_{v, Z^{(t+1),v}}; X_{v,:}^{(t)}). \tag{3}$$

Here, $f_{\mathcal{V} \rightarrow \mathcal{E}}$ and $f_{\mathcal{E} \rightarrow \mathcal{V}}$ are the key multiset functions mapping node and hyperedge features. For example, $f_{\mathcal{V} \rightarrow \mathcal{E}}(S) = \text{MLP}(\sum_{s \in S} \text{MLP}(s))$ is used in AllDeepSets. The notation $V_{e,X}$ and $E_{v,Z}$ represent multisets of node and hyperedge features, respectively. The AllSet approach updates nodes and hyperedges in the hypergraph by leveraging their features in conjunction with those of adjacent hyperedges or nodes, enabling a rich representation of the hypergraph structure. The method could differentiate node v from its multiset, allowing for sophisticated feature aggregation.

4 Methods

We introduce the SE3Set model to leverage hypergraph neural networks for capturing complex molecular interactions, integrating both 2D chemical and 3D spatial structures (Sec. 4.1). It builds upon the AllSet framework [52] and the Equiformer [26]. Upcoming sections will delve into the specifics of molecular fragmentation and the SE3Set architecture.

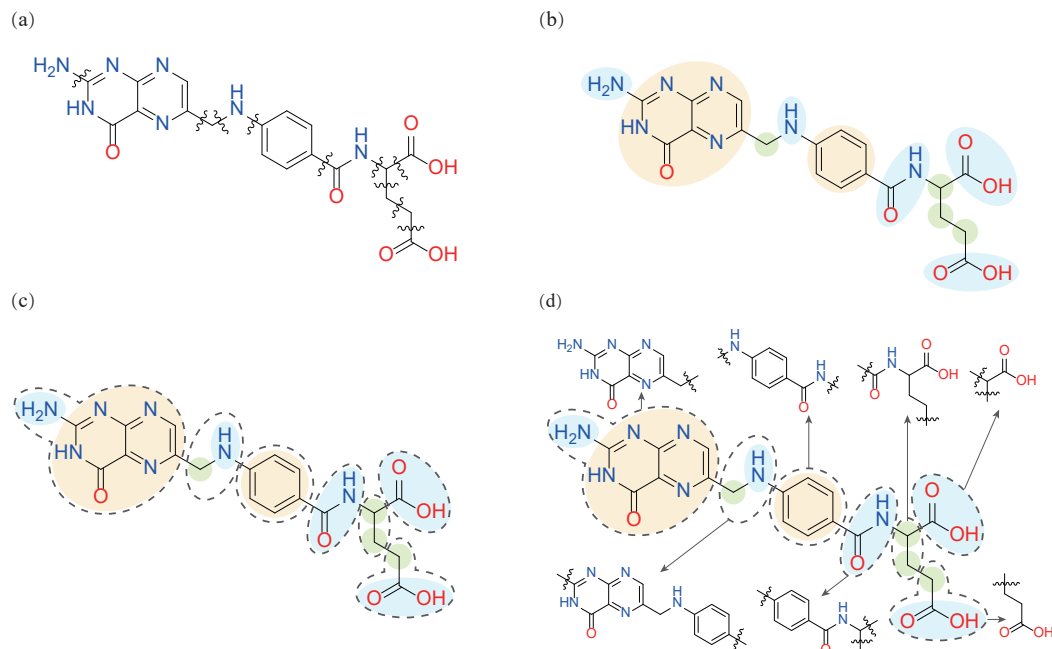


Figure 1: Folic acid fragmentation illustrated with CID 135398658 from PubChem. (a) Preprocessing to identify cleavable bonds for fragmentation. (b) Initial fragments formed using BFS, color-coded by functional groups (blue), rings (orange), and single atoms (green). (c) Fragments merged to satisfy atom count criteria, detailed in C. (d) Expansion of fragments shown with directional arrows.

4.1 Fragmentation algorithm

To harness the power of hypergraph neural networks for molecular representations, we need to map molecules onto hypergraph structures through a refined fragmentation algorithm. Our strategy intertwines molecular topology and spatial geometry to create hyperedges that capture groups of atoms, reflecting their functional and spatial characteristics. In crafting this fragmentation approach for hypergraph-based molecular representation, the methodology must adhere to a set of fundamental principles:

1. The design should merge topological chemistry with 3D structural data into a unified hypergraph representation, ensuring hyperedges accurately embody the molecule’s chemical and spatial properties.
2. Controlling fragment size is vital for the SE3Set model to balance capturing meaningful interactions and computational efficiency. Optimal fragment sizes are key for model performance and learning capabilities.
3. The fragmentation could only selectively break single bonds and must maintain functional groups and ring integrity to preserving key chemical information critical for the molecule’s properties and behavior.
4. Fragment overlap is essential to maintain functional group effects on local charge distribution and to ensure hyperedge interaction within the SE3Set model for improved molecular learning.

Before delving deeper into the specifics of our fragmentation method, it’s important to establish a foundational understanding through key definitions and concepts,

Definition 4.1. The bond order represents the multiplicity or the number of shared electron pairs that constitute a covalent bond between two atoms.

The bond order matrix \mathbf{B} is an $N \times N$ representation of bond strength between atoms in a molecule, with higher bond order values indicating stronger bonds. This symmetric matrix ($B_{ij} = B_{ji}$) is crucial for studying molecular structure and reactivity, capturing bond nuances including delocalized and resonance bonds in computational chemistry.

Our fragmentation algorithm improves molecular representations by combining bond order, functional groups, and substructures, including SMARTS-identified smaller rings and merged adjacent groups. Overcoming the drawbacks of non-overlapping fragmentation, it uses 3D spatial data and allows overlaps, preserving local effects for precise charge distribution and enhancing hypergraph neural network learning of molecular interactions.

Definition 4.2. A molecular fragment, denoted as \mathfrak{F} , is defined as a specific subset of atoms within a molecule, characterized by being a cohesive assembly of predefined substructures linked in a sequential concatenation.

Our fragmentation method meticulously dissects a given molecule into meaningful subsets of atoms, and this process unfolds through four steps (corresponding to the pipeline in Fig. 1):

1. Pre-processing by analyzing the molecule’s bond order matrix to mask high-order bonds and those within functional groups or rings, and merging adjacent functional groups for a streamlined structural representation.
2. Core substructures are delineated from the remaining bonds using a Breadth-First Search algorithm, establishing the basic units of the molecular framework.
3. These substructures are then aggregated into larger molecular fragments according to predefined rules that maintain a minimum atom count within each fragment. This step could be optional.
4. To enhance fragment connectivity, we expand each by incorporating adjacent groups, using interaction strength metrics based on interatomic distances to guide this process. Here we set the cutoff value denoted as c_w of an interaction strength metrics to intercept the extended fragment.

Furthermore, step 4 leads to a substantial computational overhead for hypergraph neural networks when processing larger molecular systems. To enhance the efficiency of our model for such expansive molecular systems, we introduce a revised strategy for step 4:

- 4* For each atom i , identify the neighboring atoms \mathcal{N}_i that fall within a specified radial cutoff r_c . A fragment \mathfrak{F} is considered to be adjacent to atom i if there is an overlap of at least one atom between \mathfrak{F} and \mathcal{N}_i . For ease of reference, the set of fragments adjacent to atom i is represented as $\mathcal{N}_i^{\mathfrak{F}}$, which implies that $\mathcal{N}_i^{\mathfrak{F}} = \{\mathfrak{F} | \mathfrak{F} \cap \mathcal{N}_i \neq \emptyset\}$.

We designate the application of step 4 as an explicit overlap and the application of step 4* as an implicit overlap. These approaches introduce nuanced variations in the mathematical expressions of our model, as reflected in the Eq. 8, Eq. 9, and Eq. 16. For the detailed step-by-step methodology, please refer to Appendix A.

4.2 SE3Set

Building upon our aforementioned fragmentation algorithm, we now turn to outline the architecture of SE3Set. SE3Set model, influenced by AllSet [52] and built on the Equiformer [26], incorporates 3D spatial equivariance in our hypergraph neural network, improving capture of many-body interactions for precise molecular structure representation. SE3Set consists of an embedding layer, attention blocks, and an output head, as shown in Fig. 2 (a).

4.2.1 Embedding

As depicted in Fig. 2 (b), the embedding block generates detailed node and hyperedge features reflecting molecular structures. Node features blend intrinsic properties with degree embeddings

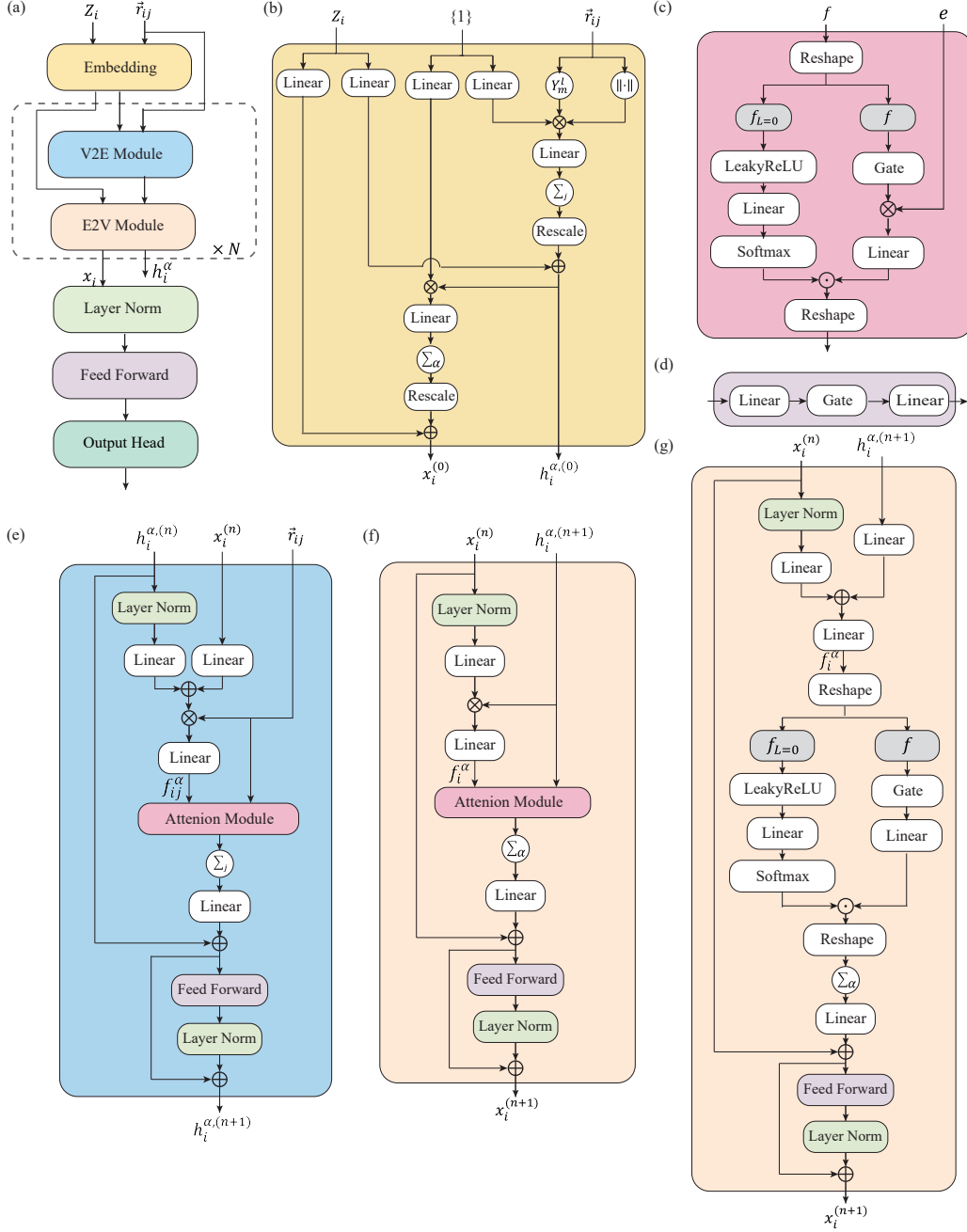


Figure 2: Overall architecture of SE3Set. (a) SE3Set begins with node and hyperedge embeddings, cycles through V2E and E2V attention modules for iterative updates, and concludes with normalization and a feed-forward block for output. (b) Embedding. Atomic numbers and position vectors are transformed into initial embeddings for nodes and hyperedges. (c) Attention Block. Merges feature sets with positional or hyperedge data for feature processing. (d) Feed-Forward Block. Enhances feature sets through a streamlined network. (e) V2E Module. Utilizes node features and their relative positions to update hyperedge features. (f) E2V Module. Employs hyperedge features to refresh node features, using tensor products (left) or summation (right) for updates. Symbols \otimes , \oplus , and \odot in figures denote depth-wise tensor product, summation, and Hadamard multiplication, respectively. h_i^α represents hyperedge features, x_i is for node features, superscript n indicates the number of updates, and \vec{r}_{ij} is the relative position vector between nodes i and j .

from connected hyperedges, while hyperedge features aggregate node embeddings. They’re mapped onto l -order SH functions for SE3 equivariance and updated separately. Hyperedges capture nodes’ positional relationships, assigning a distinct feature h_i^α to each node i in hyperedge \mathfrak{F}_α , reinforcing structural fidelity. Nodes x_i integrate hyperedge information, harmonizing uniqueness with interconnections. Attention mechanisms then refine node and hyperedge interactions for accurate molecular and structural representation.

4.2.2 Equivariant hypergraph attention blocks

As presented in Fig. 2 (c)-(f), the attention mechanism comprises two essential components: the Vertex-to-Edge (V2E) and Edge-to-Vertex (E2V) attention blocks, based on the AllSet framework [52]. The V2E block refines hyperedge features, while the E2V block updates node features, both operating with an equivariant hypergraph attention mechanism. To improve training and enable deeper network structures, we incorporate normalization layers and residual connections to prevent gradient issues. The attention module’s output passes through a feed forward block (Fig. 2 (d)), enhancing representation complexity. Node and hyperedge features maintain equivariance to molecular geometry, preserving data symmetries and the integrity of representations, thus boosting the model’s expressiveness in capturing complex structural interactions. (The concepts of irreducible representations and tensor products can be referenced in the Appendix E.)

V2E attention The SE3Set model uses geometrically invariant attention weights a_{ij} , derived from $l = 0$ irreps acting as scalars under geometric transformations. These weights are computed from scalar features $f_{ij,l=0}$ using an MLP with LeakyReLU activation and softmax normalization, reflecting node relationships within the hypergraph. Node and hyperedge features undergo non-linear transformations represented by tensor products of irreps with quantum number l . The features combine through direct tensor products (DTP), yielding non-linear values v_{ij} (Fig. 2 (c)). Hyperedge features are updated by aggregating features from connected nodes, utilizing SH and radial basis functions on hyperedge features. The model calculates initial features f_{ij}^α and V2E attention weights a_{ij}^α via MLPs, with non-linear values v_{ij}^α emerging from similar transformations.

$$t_{ij}^\alpha = (\text{Linear}(x_i) + \text{Linear}(x_j)) \quad (4)$$

$$f_{ij}^\alpha = \text{Linear}(t_{ij}^\alpha \otimes_w^{\text{DTP}} \text{SH}(\vec{r}_{ij})) \quad (5)$$

$$a_{ij}^\alpha = \text{Softmax}_j(a^\top \text{LeakyReLU}(f_{ij,l=0}^\alpha)) \quad (6)$$

$$v_{ij}^\alpha = \text{Linear}(\text{Gate}(f_{ij}^\alpha) \otimes_w^{\text{DTP}} \text{SH}(\vec{r}_{ij})) \quad (7)$$

Ultimately, the SE3Set model updates hyperedge features h_i^k by accumulating the weighted features of nodes within the same hyperedge and applying a linear transformation to the aggregated information. For the explicit overlap fragmentation method,

$$\Delta h_i^\alpha = \text{Linear} \left(\sum_{j:n_i \in \mathfrak{F}_\alpha \wedge n_j \in \mathfrak{F}_\alpha} a_{ij}^\alpha v_{ij}^\alpha \right) \quad (8)$$

where n_i denotes the node with index i and \mathfrak{F}_α denotes the fragment with index α as each fragment could be considered as a hyperedge in the hypergraph. Due to the frequent occurrence of a high number of explicitly overlapping atoms, this scenario commonly results in increased computational complexity. Consequently, when adopting the implicit overlap approach, we may opt for an equation of the form:

$$\Delta h_i^\alpha = \text{Linear} \left(\sum_{j:j \in \mathfrak{F}_\alpha \wedge \mathfrak{F}_\alpha \in \mathcal{N}_i^\mathcal{F}} a_{ij}^\alpha v_{ij}^\alpha \right) \quad (9)$$

where $\mathcal{N}_i^\mathcal{F}$ is delineated in step 4* of the implicit overlap method. This characteristic renders it a more computationally efficient scheme for Vertex-to-Edge (V2E) attention mechanisms. The detailed architecture of V2E attention block is shown in Fig. 2 (e).

E2V attention Following the V2E attention module, the E2V attention module (Fig. 2 (f)) updates node features by transforming them with a tensor product of the updated hyperedge feature, followed

by a linear layer. Attention weights are then calculated using softmax-applied, LeakyReLU-activated features, ensuring node features are refined after hyperedge updates.

$$f_i^\alpha = \text{Linear}(\text{Linear}(x_i) \otimes^{\text{DTP}} h_i^\alpha) \quad (10)$$

$$a_i^\alpha = \text{Softmax}_\alpha(a^\top \text{LeakyReLU}(f_{i,l=0}^\alpha)) \quad (11)$$

These attention weights direct the synthesis of information, culminating in the calculated value:

$$v_i^\alpha = \text{Linear}(\text{Gate}(f_i^\alpha) \otimes^{\text{DTP}} h_i^\alpha). \quad (12)$$

Furthermore, we propose an alternative method for constructing the E2V attention block as shown in Fig. 2 (g).

$$f_i^\alpha = \text{Linear}(\text{Linear}(x_i) + \text{Linear}(h_i^\alpha)) \quad (13)$$

$$a_i^\alpha = \text{Softmax}_\alpha(a^\top \text{LeakyReLU}(f_{i,l=0}^\alpha)) \quad (14)$$

$$v_i^\alpha = \text{Linear}(\text{Gate}(f_i^\alpha)) \quad (15)$$

However, practical experiments reveal that the previous method yields superior results, with detailed findings presented in Sec. 5.3.

Then the node aggregates all the hyperedge features corresponding to itself to update the node feature,

$$\text{Explicit overlap: } \Delta x_i = \text{Linear} \left(\sum_{\alpha: i \in \mathfrak{F}_\alpha} a_i^\alpha v_i^\alpha \right), \quad (16)$$

$$\text{Implicit overlap: } \Delta x_i = \text{Linear} \left(\sum_{\alpha: \mathfrak{F}_\alpha \in \mathcal{N}_i^{\mathcal{F}}} a_i^\alpha v_i^\alpha \right) \quad (17)$$

4.2.3 Output head

The SE3Set model employs node features to generate predictions, using a feed-forward network to transform these features into the target label’s irreps dimension. A summation strategy aggregates node features into a single hypergraph-level representation, which is then processed by a linear layer to output the model’s final predictions.

5 Results

We tested our equivariant hypergraph neural network on QM9 [55, 56], MD17 [57] (see Appendix F), and MD22 [58] to assess its molecular representation learning. QM9 and MD17 gauge small molecule property prediction, while MD22 evaluates larger systems with complex many-body interactions [22]. An ablation study was also conducted to pinpoint the contributions of fragmentation and architecture to our method’s performance, offering insights into the network’s efficacy and areas for enhancement.

Table 1: A comparative analysis was performed to assess the Mean Absolute Errors (MAEs) on the QM9 dataset when training SE3Set on a configuration comprising 110,000 training samples and 1,000 validation samples. Bolding shows the best model and underlining shows the second best model and the underlining tilde shows third best model.

	UNIT	SCHNET	DIMENET++	PAINN	SPHERESET	COMENET	ET	ALLEGRO	VISNET	QUINNET	EQUIFORMER	SE3SET
μ	D	0.033	0.030	0.012	0.026	0.0245	<u>0.011</u>	-	0.010	0.771	<u>0.011</u>	<u>0.011</u>
α	a_0^2	0.235	<u>0.044</u>	<u>0.045</u>	0.046	0.0452	0.059	-	0.041	0.047	<u>0.046</u>	<u>0.045</u>
HOMO	meV	41	<u>25</u>	<u>20</u>	23	23	20	-	<u>17.3</u>	20.4	15	15
LUMO	meV	34	20	28	18	20	18	-	<u>14.8</u>	17.6	<u>14</u>	13
GAP	meV	63	33	46	32	32	36	-	31.7	28.2	<u>30</u>	<u>29</u>
R^2	a_0^2	0.073	0.331	<u>0.066</u>	0.292	0.259	<u>0.033</u>	-	0.030	0.194	0.251	0.197
ZPVE	meV	1.70	<u>1.21</u>	<u>1.28</u>	1.12	<u>1.20</u>	1.84	-	1.56	1.26	1.40	1.40
U_0	meV	14	6	5.85	6	6.59	6.15	<u>4.7</u>	4.23	7.6	6.59	<u>5.74</u>
U	meV	19	6	5.83	7	6.82	6.38	<u>4.4</u>	4.25	8.4	6.74	<u>5.69</u>
H	meV	14	7	5.98	6	6.86	6.16	4.4	<u>4.52</u>	7.8	6.63	<u>5.70</u>
G	meV	14	8	7.35	8	7.98	7.62	5.7	<u>5.86</u>	8.5	7.63	<u>6.63</u>
C_v	$\frac{\text{kcal}}{\text{mol}\cdot\text{K}}$	0.033	<u>0.023</u>	0.024	0.021	0.024	0.026	-	<u>0.023</u>	0.024	<u>0.023</u>	0.025

5.1 QM9

The QM9 dataset [55, 56] consists of 134k small organic molecules calculated at the B3LYP/6-31G(2df, p) level. SE3Set, after training on 110k QM9 molecules and validation on 10k, achieves low mean absolute errors (MAEs) in 12 tasks, performing on par with leading models, as detailed in Table 1. In small molecular systems, higher-order many-body interactions are less pronounced, and as a result, SE3Set does not significantly outperform other state-of-the-art (SOTA) models.

Table 2: A comparison of Mean Absolute Errors (MAEs) across various benchmarked models. SE3Set is trained on the five molecules of MD22 dataset with specific number of training/validation. Bolding shows the best model and underlining shows the second best model. The improvements column shows the improvement of our model over the previous SOTA model in percentage terms. The MAEs reflect the precision of energy predictions in units of kcal/mol and forces in units of kcal/(mol·Å). The results of TorchMD-Net, Allegro, and Equiformer are extracted from Ref. [59]

MOLECULE	# TRAIN/VAL		SGDML	TORCHMD-NET	ALLEGRO	MACE	EQUIFORMER	VISNET	QUINNET	EQUIFORMER-LSRM	VISNET-LSRM	SE3SET	IMPROVEMENTS
AC-ALA3-NHME	5500/500	ENERGY	0.3902	0.1121	0.1019	<u>0.0620</u>	0.0828	0.0796	0.084	0.0780	0.0654	0.0499	19.5%
		FORCE	0.7968	0.1879	0.1068	0.0876	0.0804	0.0972	<u>0.0681</u>	0.0877	0.0902	0.0545	20.0%
DHA	7500/500	ENERGY	1.3117	0.1205	0.1153	0.1317	0.1788	0.1526	0.12	0.0878	<u>0.0873</u>	0.0826	5.4%
		FORCE	0.7474	0.1209	0.0732	0.0646	<u>0.0506</u>	0.0668	0.0515	0.0534	0.0598	0.0360	28.9%
STACHYOSE	7500/500	ENERGY	4.0497	0.1393	0.2485	0.1244	0.1404	0.1283	0.23	0.1252	<u>0.1055</u>	0.0762	27.8%
		FORCE	0.6744	0.1921	0.0971	0.0876	0.0635	0.0869	<u>0.0543</u>	0.0632	0.0767	0.0424	21.9%
AT-AT	2500/500	ENERGY	0.7235	0.1120	0.1428	0.1093	0.1309	0.1688	0.14	0.1007	<u>0.0722</u>	0.0585	24.2%
		FORCE	0.6911	0.2036	0.0952	0.0992	0.0960	0.1070	<u>0.0687</u>	0.0811	0.0781	0.0556	19.1%
AT-AT-CG-CG	1500/500	ENERGY	1.3885	0.2072	0.3933	0.1578	0.1510	0.1995	0.38	0.1335	<u>0.1135</u>	0.1002	11.7%
		FORCE	0.7028	0.3259	0.1280	0.1153	0.1252	0.1563	0.1273	0.1065	<u>0.1063</u>	0.0825	22.4%

5.2 MD22

Recognizing the prominence of higher-order many-body interactions in larger molecules [22], SE3Set was tested on the comprehensive MD22 dataset [58]. This dataset spans four classes of biomolecules and supramolecules, from a 42-atom peptide to a 370-atom nanotube, with high-resolution sampling at 400-500 K using the PBE+MBD [60, 61] framework for energy and force computations. Our fragmentation method, which maintains functional groups and rings, selectively excludes structures like the Buckyball catcher and Double-walled nanotube from MD22, thus concentrating on the other five molecular types. As Table 2 shows, SE3Set outperforms other SOTA models in these cases, reducing MAEs by an average of 20%, underscoring its exceptional ability to capture molecular intricacies. Moreover, our results indicate that incorporating higher-order many-body interactions is crucial for representing the non-local features of larger molecules within the MD22 dataset.

5.3 Ablation studies

To better understand SE3Set, we conduct ablation studies focusing on fragmentation and model architecture. We explore how different fragmentation techniques affects SE3Set’s training and compare with the non-overlapping BRICS [62, 63] strategy. As Fig. 3 indicates, tests on QM9’s homo energy task showed SE3Set’s robustness to c_w variations in fragmentation method. Our method surpasses BRICS demonstrates the importance of hyperedge interaction. Furthermore, we performed ablation studies on the model architecture. Among two design variants in the E2V attention section, the one using tensor product interactions between nodes and hyperedges proved superior, emphasizing the value of our tensor product-based mechanism and architecture design in enhancing molecular property predictions. Additionally, a 6-layer SE3Set model outperformed its 3-layer counterpart.

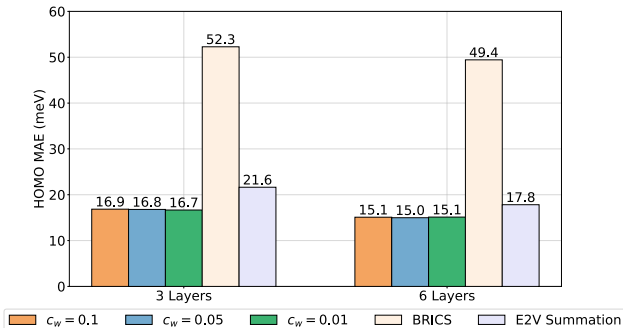


Figure 3: Ablation studies on the QM9 dataset’s HOMO task (units: meV). The variable c_w represents the threshold for expansion in the fourth step of fragmentation, guided by the fragment bond order defined in Eq. 18. The term BRICS denotes another fragmentation method implemented in RDKit. Additionally, the E2V summation refers to the architectural framework specified from Eq. 13 to Eq. 15.

6 Conclusion

In conclusion, this study demonstrate the efficacy of SE3Set, a cutting-edge hypergraph neural network architecture, in the realm of molecular representation learning. By meticulously crafting a fragmentation method that coalesces two-dimensional chemical knowledge with three-dimensional spatial information, we establish a robust foundation for constructing hypergraphs that faithfully capture the complex nature of molecular structures. The SE3Set architecture, drawing inspiration from the AllSet framework and the Equiformer, adeptly processing these hypergraphs and preserving the essential invariances and symmetries. SE3Set demonstrates performance comparable to SOTA models in small molecular systems and significantly outperforms SOTA models in large molecular systems where higher-order many-body interactions are pronounced. The results of our research affirm the potential of SE3Set to model high-order many-body interactions, providing a powerful tool for molecular representation.

References

- [1] Jonathan P Mathews and Alan L Chaffee. The molecular representations of coal—a review. *Fuel*, 96:1–14, 2012.
- [2] Laurianne David, Amol Thakkar, Rocío Mercado, and Ola Engkvist. Molecular representations in AI-driven drug discovery: a review and practical guide. *J. Cheminform.*, 12(1):1–22, 2020.
- [3] Daniel S Wigh, Jonathan M Goodman, and Alexei A Lapkin. A review of molecular representation in the age of machine learning. *Wiley Interdiscip. Rev. Comput. Mol. Sci.*, 12(5):e1603, 2022.
- [4] Denis Fourches, Eugene Muratov, and Alexander Tropsha. Trust, but verify: on the importance of chemical structure curation in cheminformatics and qsar modeling research. *J. Chem. Inf. Model.*, 50(7):1189, 2010.
- [5] Jie Zhou, Ganqu Cui, Shengding Hu, Zhengyan Zhang, Cheng Yang, Zhiyuan Liu, Lifeng Wang, Changcheng Li, and Maosong Sun. Graph neural networks: A review of methods and applications. *AI open*, 1:57–81, 2020.
- [6] Zonghan Wu, Shirui Pan, Fengwen Chen, Guodong Long, Chengqi Zhang, and S Yu Philip. A comprehensive survey on graph neural networks. *IEEE Trans. Neural. Netw. Learn. Syst.*, 32(1):4–24, 2020.
- [7] Kien Do, Truyen Tran, and Svetha Venkatesh. Graph transformation policy network for chemical reaction prediction. In *Proceedings of the 25th ACM SIGKDD international conference on knowledge discovery & data mining*, pages 750–760, 2019.
- [8] Jiacheng Xiong, Zhaoping Xiong, Kaixian Chen, Hualiang Jiang, and Mingyue Zheng. Graph neural networks for automated de novo drug design. *Drug Discov. Today*, 26(6):1382–1393, 2021.
- [9] Patrick Reiser, Marlen Neubert, André Eberhard, Luca Torresi, Chen Zhou, Chen Shao, Housam Metni, Clint van Hoesel, Henrik Schopmans, Timo Sommer, et al. Graph neural networks for materials science and chemistry. *Commun. Mater.*, 3(1):93, 2022.
- [10] Justin Gilmer, Samuel S Schoenholz, Patrick F Riley, Oriol Vinyals, and George E Dahl. Neural message passing for quantum chemistry. In *International conference on machine learning*, pages 1263–1272. PMLR, 2017.
- [11] Jonathan Godwin, Michael Schaarschmidt, Alexander L Gaunt, Alvaro Sanchez-Gonzalez, Yulia Rubanova, Petar Veličković, James Kirkpatrick, and Peter Battaglia. Simple GNN regularisation for 3D molecular property prediction and beyond. In *International Conference on Learning Representations*, 2021.
- [12] T Konstantin Rusch, Michael M Bronstein, and Siddhartha Mishra. A survey on oversmoothing in graph neural networks. Preprint at <http://arxiv.org/abs/2303.10993>, 2023.
- [13] Johannes Gasteiger, Janek Groß, and Stephan Günnemann. Directional message passing for molecular graphs. In *International Conference on Learning Representations*, 2019.
- [14] Kristof Schütt, Oliver Unke, and Michael Gastegger. Equivariant message passing for the prediction of tensorial properties and molecular spectra. In *International Conference on Machine Learning*, pages 9377–9388. PMLR, 2021.

- [15] Simon Batzner, Albert Musaelian, Lixin Sun, Mario Geiger, Jonathan P Mailoa, Mordechai Kornbluth, Nicola Molinari, Tess E Smidt, and Boris Kozinsky. E (3)-equivariant graph neural networks for data-efficient and accurate interatomic potentials. *Nat. Commun.*, 13(1):2453, 2022.
- [16] Johannes Gasteiger, Shankari Giri, Johannes T Margraf, and Stephan Günnemann. Fast and uncertainty-aware directional message passing for non-equilibrium molecules. *Preprint at <http://arxiv.org/abs/2011.14115>*, 2020.
- [17] Johannes Gasteiger, Florian Becker, and Stephan Günnemann. Gemnet: Universal directional graph neural networks for molecules. *Advances in Neural Information Processing Systems*, 34:6790–6802, 2021.
- [18] Philipp Thölke and Gianni De Fabritiis. Equivariant transformers for neural network based molecular potentials. In *International Conference on Learning Representations*, 2021.
- [19] Ilyes Batatia, David P Kovacs, Gregor Simm, Christoph Ortner, and Gábor Csányi. MACE: Higher order equivariant message passing neural networks for fast and accurate force fields. *Advances in Neural Information Processing Systems*, 35:11423–11436, 2022.
- [20] Albert Musaelian, Simon Batzner, Anders Johansson, Lixin Sun, Cameron J Owen, Mordechai Kornbluth, and Boris Kozinsky. Learning local equivariant representations for large-scale atomistic dynamics. *Nat. Commun.*, 14(1):579, 2023.
- [21] Yusong Wang, Tong Wang, Shaoning Li, Xinheng He, Mingyu Li, Zun Wang, Nanning Zheng, Bin Shao, and Tie-Yan Liu. Enhancing geometric representations for molecules with equivariant vector-scalar interactive message passing. *Nat. Commun.*, 15(1):313, 2024.
- [22] Zun Wang, Guoqing Liu, Yichi Zhou, Tong Wang, and Bin Shao. Efficiently incorporating quintuple interactions into geometric deep learning force fields. In *Thirty-seventh Conference on Neural Information Processing Systems*, 2023.
- [23] Nathaniel Thomas, Tess Smidt, Steven Kearnes, Lusann Yang, Li Li, Kai Kohlhoff, and Patrick Riley. Tensor field networks: Rotation-and translation-equivariant neural networks for 3d point clouds. *Preprint at <http://arxiv.org/abs/1802.08219>*, 2018.
- [24] Brandon Anderson, Truong Son Hy, and Risi Kondor. Cormorant: Covariant molecular neural networks. *Advances in neural information processing systems*, 32, 2019.
- [25] Fabian Fuchs, Daniel Worrall, Volker Fischer, and Max Welling. SE (3)-transformers: 3D Roto-translation equivariant attention networks. *Advances in Neural Information Processing Systems*, 33:1970–1981, 2020.
- [26] Yi-Lun Liao and Tess Smidt. Equiformer: Equivariant graph attention transformer for 3D atomistic graphs. In *The Eleventh International Conference on Learning Representations*, 2022.
- [27] Yi-Lun Liao, Brandon Wood, Abhishek Das, and Tess Smidt. EquiformerV2: Improved equivariant transformer for scaling to higher-degree representations. *Preprint at <http://arxiv.org/abs/2306.12059>*, 2023.
- [28] Kristof Schütt, Pieter-Jan Kindermans, Huziel Enoc Saucedo Felix, Stefan Chmiela, Alexandre Tkatchenko, and Klaus-Robert Müller. Schnet: A continuous-filter convolutional neural network for modeling quantum interactions. *Advances in neural information processing systems*, 30, 2017.
- [29] P-J Kindermans and K-R Müller. Schnet—a deep learning architecture for molecules and materials. *J. Chem. Phys.*, 148(24), 2018.
- [30] Benjamin Coors, Alexandru Paul Condurache, and Andreas Geiger. SphereNet: Learning spherical representations for detection and classification in omnidirectional images. In *Proceedings of the European conference on computer vision (ECCV)*, pages 518–533, 2018.
- [31] Limei Wang, Yi Liu, Yuchao Lin, Haoran Liu, and Shuiwang Ji. ComENet: Towards complete and efficient message passing for 3D molecular graphs. In Alice H. Oh, Alekh Agarwal, Danielle Belgrave, and Kyunghyun Cho, editors, *Advances in Neural Information Processing Systems*, 2022.
- [32] Sameer Agarwal, Jongwoo Lim, Lihi Zelnik-Manor, Pietro Perona, David Kriegman, and Serge Belongie. Beyond pairwise clustering. In *2005 IEEE Computer Society Conference on Computer Vision and Pattern Recognition (CVPR’05)*, volume 2, pages 838–845. IEEE, 2005.

- [33] Dengyong Zhou, Jiayuan Huang, and Bernhard Schölkopf. Learning with hypergraphs: Clustering, classification, and embedding. *Advances in neural information processing systems*, 19, 2006.
- [34] Guoyin Li, Liqun Qi, and Gaohang Yu. The Z-eigenvalues of a symmetric tensor and its application to spectral hypergraph theory. *Numer. Linear Algebra Appl.*, 20(6):1001–1029, 2013.
- [35] Kelly J Pearson and Tan Zhang. On spectral hypergraph theory of the adjacency tensor. *Graphs Combin.*, 30:1233–1248, 2014.
- [36] Austin R Benson, David F Gleich, and Lek-Heng Lim. The spacey random walk: A stochastic process for higher-order data. *SIAM Rev.*, 59(2):321–345, 2017.
- [37] Eli Chien, Pan Li, and Olgica Milenkovic. Landing probabilities of random walks for seed-set expansion in hypergraphs. In *2021 IEEE Information Theory Workshop (ITW)*, pages 1–6. IEEE, 2021.
- [38] Francesco Tudisco, Austin R Benson, and Konstantin Prokopychik. Nonlinear higher-order label spreading. In *Proceedings of the Web Conference 2021*, pages 2402–2413, 2021.
- [39] Jinwoo Kim, Saeyoon Oh, and Seunghoon Hong. Transformers generalize deepsets and can be extended to graphs & hypergraphs. *Advances in Neural Information Processing Systems*, 34:28016–28028, 2021.
- [40] Jinwoo Kim, Saeyoon Oh, Sungjun Cho, and Seunghoon Hong. Equivariant hypergraph neural networks. In *European Conference on Computer Vision*, pages 86–103. Springer, 2022.
- [41] Shicheng Cui, Qianmu Li, Deqiang Li, Zhichao Lian, Jun Hou, et al. Hyper-mol: Molecular representation learning via fingerprint-based hypergraph. *Comput. Intell. Neurosci.*, 2023, 2023.
- [42] Mohammadamin Tavakoli, Alexander Shmakov, Francesco Ceccarelli, and Pierre Baldi. Rxn hypergraph: a hypergraph attention model for chemical reaction representation. *Preprint at <http://arxiv.org/abs/2201.01196>*, 2022.
- [43] Hiroshi Kajino. Molecular hypergraph grammar with its application to molecular optimization. In *International Conference on Machine Learning*, pages 3183–3191. PMLR, 2019.
- [44] Eliya Nachmani and Lior Wolf. Molecule property prediction and classification with graph hypernetworks. *Preprint at <http://arxiv.org/abs/2002.00240>*, 2020.
- [45] Fangying Chen, Junyoung Park, and Jinkyoo Park. A hypergraph convolutional neural network for molecular properties prediction using functional group. *Preprint at <http://arxiv.org/abs/2106.01028>*, 2021.
- [46] Junwu Chen and Philippe Schwaller. Molecular hypergraph neural networks. *Preprint at <http://arxiv.org/abs/2312.13136>*, 2023.
- [47] Mark S Gordon, Dmitri G Fedorov, Spencer R Pruitt, and Lyudmila V Slipchenko. Fragmentation methods: A route to accurate calculations on large systems. *Chem. Rev.*, 112(1):632–672, 2012.
- [48] Michael A Collins and Ryan PA Bettens. Energy-based molecular fragmentation methods. *Chem. Rev.*, 115(12):5607–5642, 2015.
- [49] Boxin Du, Changhe Yuan, Robert Barton, Tal Neiman, and Hanghang Tong. Hypergraph pre-training with graph neural networks. *Preprint at <http://arxiv.org/abs/2105.10862>*, 2021.
- [50] Seojin Kim, Jaehyun Nam, Junsu Kim, Hankook Lee, Sungsoo Ahn, and Jinwoo Shin. Contrastive learning of molecular representation with fragmented views. 2022.
- [51] Kha-Dinh Luong and Ambuj Singh. Fragment-based pretraining and finetuning on molecular graphs. *Preprint at <http://arxiv.org/abs/2310.03274>*, 2023.
- [52] Eli Chien, Chao Pan, Jianhao Peng, and Olgica Milenkovic. You are AllSet: A multiset function framework for hypergraph neural networks. In *International Conference on Learning Representations*, 2021.
- [53] Manzil Zaheer, Satwik Kottur, Siamak Ravanbakhsh, Barnabas Poczos, Russ R Salakhutdinov, and Alexander J Smola. Deep sets. *Advances in neural information processing systems*, 30, 2017.

- [54] Juho Lee, Yoonho Lee, Jungtaek Kim, Adam Kosior, Seungjin Choi, and Yee Whye Teh. Set transformer: A framework for attention-based permutation-invariant neural networks. In International conference on machine learning, pages 3744–3753. PMLR, 2019.
- [55] Lars Ruddigkeit, Ruud Van Deursen, Lorenz C Blum, and Jean-Louis Reymond. Enumeration of 166 billion organic small molecules in the chemical universe database GDB-17. J. Chem. Inf. Model., 52(11):2864–2875, 2012.
- [56] Raghunathan Ramakrishnan, Pavlo O Dral, Matthias Rupp, and O Anatole Von Lilienfeld. Quantum chemistry structures and properties of 134 kilo molecules. Sci. Data, 1(1):1–7, 2014.
- [57] Stefan Chmiela, Alexandre Tkatchenko, Huziel E Sauceda, Igor Poltavsky, Kristof T Schütt, and Klaus-Robert Müller. Machine learning of accurate energy-conserving molecular force fields. Sci. Adv., 3(5):e1603015, 2017.
- [58] Stefan Chmiela, Valentin Vassilev-Galindo, Oliver T Unke, Adil Kabylda, Huziel E Sauceda, Alexandre Tkatchenko, and Klaus-Robert Müller. Accurate global machine learning force fields for molecules with hundreds of atoms. Science Advances, 9(2):eadf0873, 2023.
- [59] Yunyang Li, Yusong Wang, Lin Huang, Han Yang, Xinran Wei, Jia Zhang, Tong Wang, Zun Wang, Bin Shao, and Tie-Yan Liu. Long-short-range message-passing: A physics-informed framework to capture non-local interaction for scalable molecular dynamics simulation. In The Twelfth International Conference on Learning Representations, 2024.
- [60] John P Perdew, Kieron Burke, and Matthias Ernzerhof. Generalized gradient approximation made simple. Phys. Rev. Lett., 77(18):3865, 1996.
- [61] Alexandre Tkatchenko, Robert A DiStasio Jr, Roberto Car, and Matthias Scheffler. Accurate and efficient method for many-body van der Waals interactions. Phys. Rev. Lett., 108(23):236402, 2012.
- [62] Jörg Degen, Christof Wegscheid-Gerlach, Andrea Zaliani, and Matthias Rarey. On the art of compiling and using ‘drug-like’ chemical fragment spaces. ChemMedChem: Chemistry Enabling Drug Discovery, 3(10):1503–1507, 2008.
- [63] Greg Landrum, Paolo Tosco, Brian Kelley, sriniker, gedec, NadineSchneider, Riccardo Vianello, Ric, Andrew Dalke, Brian Cole, AlexanderSavelyev, Matt Swain, Samo Turk, Dan N, Alain Vaucher, Eisuke Kawashima, Maciej Wójcikowski, Daniel Probst, guillaume godin, David Cosgrove, Axel Pahl, JP, Francois Berenger, strets123, JLVarjo, Noel O’Boyle, Patrick Fuller, Jan Holst Jensen, Gianluca Sforna, and DoliathGavid. rdkit/rdkit: 2020_03_1 (q1 2020) release, March 2020.
- [64] György Lendvai. On the correlation of bond order and bond length. J. Mol. Struct., 501:389–393, 2000.
- [65] Adam J. Bridgeman and Christopher J Empson. Bond orders between molecular fragments. Chemistry, 12 8:2252–62, 2006.
- [66] David L Mobley, Caitlin C Bannan, Andrea Rizzi, Christopher I Bayly, John D Chodera, Victoria T Lim, Nathan M Lim, Kyle A Beauchamp, David R Slochower, Michael R Shirts, et al. Escaping atom types in force fields using direct chemical perception. J. Chem. Theory Comput., 14(11):6076–6092, 2018.
- [67] Jeff Wagner, Matt Thompson, David L. Mobley, John Chodera, Caitlin Bannan, Andrea Rizzi, trevorgokey, David L. Dotson, Josh A. Mitchell, jaimergp, Camila, Pavan Behara, Christopher Bayly, JoshHorton, Iván Pulido, Lily Wang, Victoria Lim, Sukanya Sasmal, SimonBoothroyd, Andrew Dalke, Daniel Smith, Brent Westbrook, Josh Horton, Lee-Ping Wang, Richard Gowers, Ziyuan Zhao, Connor Davel, and Yutong Zhao. openforcefield/openff-toolkit: 0.15.1. Testing updates, January 2024.
- [68] Matthias Fey and Jan Eric Lenssen. Fast graph representation learning with pytorch geometric. Preprint at <http://arxiv.org/abs/1903.02428>, 2019.

Appendix

A Details of fragmentation steps

Based on the design principles in Sec. 4.1, the detailed step-by-step methodology of explicit overlap fragmentation method is shown as follows,

1. The pre-processing step begins by analyzing the given molecule through its bond order matrix, denoted as B . Identify and mask bonds that are part of functional groups or rings, as well as those with a bond order of $B_{ij} \geq 2$. Functional groups are then identified using predefined SMARTS patterns for accurate matching. To achieve a more generalized representation of functional groups, topologically adjacent functional groups are merged into a single entity. This aggregation allows to focus on specific subfunctional groups that are of particular interest, simplifying the complexity of the molecular structure for subsequent analysis.
2. Following the masking of selected bonds, the Breadth-First Search (BFS) algorithm is employed to reconstruct the substructures, denoted as $\{\mathfrak{S}\}$, from the remaining unmasked bonds. These groups represent the core structural units of the molecule as discussed at the outset of this section.
3. Consolidate the previously identified groups $\{\mathfrak{S}\}$ into larger molecular fragments, applying a set of predefined rules to guide the merging process. These rules are meticulously designed to ensure that each resulting fragment, now denoted as $\{\mathfrak{F}\}$, contains at least a minimum specified number of atoms. For a comprehensive understanding of the merging criteria, one can refer to the detailed rules outlined in C.
4. Extend each fragment $\{\mathfrak{F}\}$ by incorporating adjacent groups from $\{\mathfrak{S}\}$ to enrich the connectivity between molecular fragments, thus intentionally creating regions of overlap among the fragments. This expansion is controlled by a cutoff threshold, denoted as c_w , which is typically a function based on interatomic distances. the fragment bond order [64, 65], symbolized by W_{fs} , is used to quantitatively assess the interaction strength between a fragment \mathfrak{F}_i and an adjacent substructure \mathfrak{S}_j . This method reflects the interaction strength based on the proximity of atoms in different fragments, expressed by the following equation:

$$W_{fs} = \sum_{i \in \mathfrak{F}_f, j \in \mathfrak{S}_s} \exp\left(-\frac{(d_{ij} - d_{ij}^e) \cdot d_{ij}^e}{(0.25 \text{ \AA})^2}\right), \quad (18)$$

where d_{ij} represents the interatomic distance between atoms i and j , and d_{ij}^e stands for the equilibrium distance typically expected for such a bond. This equation is utilized to determine which substructures should be included in the expansion of a fragment, based on the strength of their interactions as governed by the distance function. Additionally, in alignment with Pauling's concept of "chemist's bond order" [64], an alternative method is introduced to calculate the bond order using a single exponential function,

$$W_{fs} = \sum_{i \in \mathfrak{F}_f, j \in \mathfrak{S}_s} \exp(-(d_{ij} - d_{ij}^e)), \quad (19)$$

where W_{fs} encapsulates the bond order between atoms belonging to a fragment \mathfrak{F}_f and a substructure \mathfrak{S}_s . In this context, d_{ij} signifies the actual measured distance between atom i and atom j . The term d_{ij}^e refers to the theoretical equilibrium covalent bond length, which is estimated by summing the empirical covalent radii of the two atoms involved, given by:

$$d_{ij}^e = r_{z_i} + r_{z_j}, \quad (20)$$

where r_{z_i} is the empirical covalent radius of an atom with atomic number z_i . This function provides a simplified yet effective representation of bond order, allowing us to gauge the bonding interactions within the molecular structure with respect to the proximity of the atoms.

The implicit overlap fragmentation method only change the step 4, the details of the changed fourth step has been spelled out in 4.1.

B Functional groups SMARTS

In the initial phase of our fragmentation approach, we identify functional groups using the SMARTS pattern matching language. In Table 3, we present the complete list of SMARTS patterns utilized, which have been expanded upon from the default set found within the Open Force Field toolkit [66, 67] (accessible at: <https://github.com/openforcefield/openff-fragmenter/blob/main/openff/fragmenter/data/default-functional-groups.json>).

Table 3: SMARTS patterns for functional groups employed in the preprocessing stage of fragmentation.

FUNCTIONAL GROUPS NAME	SMARTS
HYDRAZINE	[NX3:1][NX3:2]
HYDRAZONE	[NX3:1][NX2:2]
NITRIC OXIDE	[N:1]-[O:2]
AMIDE	[#7:1][#6:2](=[#8:3]), [NX3:1][CX3:2](=[OX1:3])[NX3:4]
AMIDE NEGATIVE ION	[#7:1][#6:2](-[O:-3])
ALDEHYDE	[CX3H1:1](=[O:2])[#6:3]
SULFOXIDE	[#16X3:1]=[OX1:2], [#16X3+:1][OX1:-2]
SULFONYL	[#16X4:1](=[OX1:2])=[OX1:3]
SULFINIC ACID	[#16X3:1](=[OX1:2])[OX2H,OX1H0:-3]
SULFONIC ACID	[#16X4:1](=[OX1:2])(=[OX1:3])[OX2H,OX1H0:-4]
SULFINAMIDE	[#16X4:1](=[OX1:2])(=[OX1:3])([NX3R0:4])
PHOSPHINE OXIDE	[PX4:1](=[OX1:2])([#6:3])([#6:4])([#6:5])
PHOSPHONATE	[P:1](=[OX1:2])([OX2H,OX1:-3])([OX2H,OX1:-4])
PHOSPHATE	[PX4:1](=[OX1:2])([#8:3])([#8:4])([#8:5])
CARBOXYLIC ACID	[CX3:1](=[O:2])[OX1H0-,OX2H1:3]
NITRO	[NX3+:1](=[O:2])[O:-3], [NX3:1](=[O:2])=[O:3]
ESTER	[CX3:1](=[O:2])[OX2H0:3]
TRI-HALIDE	[#6:1]([F,CL,I,Br:2])([F,CL,I,Br:3])([F,CL,I,Br:4])
HYDROXYL	[#8:1]-[#1:2]

C Merge process of fragmentation

During the third step of our fragmentation method, we introduce a strategy to enlarge substructures, ensuring that each initial fragment contains at least n_{\min} atoms, with n_{\min} being a predefined integer. To maintain permutation invariance for a molecule, we incorporate weights, W_{fs} , to guide the sequence of merging. The process is outlined in the pseudocode (Algorithm 1). The calculation of W is based on either Eq. 18 or Eq. 19. By considering the sum of bond orders to other groups, we assess each group’s centrality. The groups are then ordered first by the number of atoms they contain, followed by the summation of their bond orders, ensuring that the fragmentation merge process is permutation invariant when following this specified sequence. The algorithm then assists smaller groups in merging with others to achieve a size of at least n_{\min} atoms. Initially, we consider topologically adjacent groups with the fewest atoms. If a target group lacks topological neighbors, we proceed to merge based on the bond order from W . We introduce a threshold c_{is} that allows a group to remain isolated if it is significantly distant from others. It should be noted that isolated groups may not meet the minimum atom number requirement; however, they could be further expanded in the subsequent fragmentation step, depending on the chosen thresholds for c_{is} and c_w (refer to Sec. 4.1). Overall, this algorithm ensures a permutation invariant merging process.

D Distribution of fragmentation dataset

Different parameters used in the fragmentation process can lead to a variety of hyperedges, which in turn result in distinct hypergraphs utilized for training our model. To illustrate the variances attributed to different fragmentation parameters or methods (such as BRICS implemented in RDKit [62, 63]), we use the QM9 dataset [55, 56] to demonstrate how the data distributions attached to hypergraphs may change.

Algorithm 1 Pseudo code of fragmentation merge step.

Input: groups $\{\mathfrak{G}\}$, minimum atoms number n_{\min} , maximum atoms number n_{\max} , Topological bond order matrix B , isolated threshold c_{is}

$m = |\{\mathfrak{G}\}|$

Isolate groups $\{\mathfrak{G}^J\} = \{\}$

Calculate fragmentation bond order matrix $W_{\mathfrak{G}_i\mathfrak{G}_j}$.

Sort $\{\mathfrak{G}\}$ in descending order based on the following attributes: number of atoms, $\sum_{\mathfrak{G}', \mathfrak{G}'' \neq \mathfrak{G}} W_{\mathfrak{G}\mathfrak{G}'}$.

repeat

 Pop last fragment as \mathfrak{G}_k from $\{\mathfrak{G}\}$

for $i = m - 1$ **to** 1 **do**

$a = \text{MAX_INT}, \text{merge_idx} = -1$

if any $B_{ij} \geq 1, i \in \mathfrak{G}_i, j \in \mathfrak{G}_k$ **and** $|\mathfrak{G}_i| < a$ **and** $a + |\mathfrak{G}_i| \leq n_{\max}$ **then**

$a = |\mathfrak{G}_i|, \text{merge_idx} = i$

end if

end for

if $\text{merge_idx} == -1$ **then**

for $i = m - 1$ **to** 1 **do**

if any $W_{\mathfrak{G}_i\mathfrak{G}_k} \geq c_{is}$ **and** $|\mathfrak{G}_i| < a$ **then**

$a = |\mathfrak{G}_i|, \text{merge_idx} = -1$

end if

end for

end if

if $\text{merge_idx} \neq -1$ **then**

 Merge \mathfrak{G}_k to $\mathfrak{G}_{\text{merge_idx}}$

 Resort $\{\mathfrak{G}\}$ by the same priority and update W .

else

 Add $\{\mathfrak{G}_k\}$ to $\{\mathfrak{G}^J\}$

end if

until $|\{\mathfrak{G}_k\}| \geq n_{\min}$

$\{\mathfrak{F}\} = \{\mathfrak{G}\} \cup \{\mathfrak{G}^J\}$

The impact of adjusting fragmentation parameters on the composition of hyperedges can be observed in Fig. 4. Altering the expansion threshold c_w within a certain range has a minimal effect on fragment expansion. However, when utilizing the Lendvay bond order (Eq. 18), fragments tend to comprise fewer atoms compared to when using the Exponential bond order (Eq. 19). This difference is likely due to the more gradual decline in the exponential function, which results in a greater cumulative contribution to the weights W_{fs} .

Our ablation study (Sec. 5.3) also includes a comparison with the BRICS fragmentation method. Fragments generated by the BRICS method are observed to contain significantly fewer atoms since this approach does not create overlapping regions between different fragments.

E Concepts of irreps features and tensor product

Irreps features The SE3Set model utilizes the special orthogonal group $\text{SO}(3)$ to capture three-dimensional rotational symmetries in molecular structures. This approach is similar to Equiformer [26, 27]. It employs irreducible representations (irreps) of $\text{SO}(3)$, parameterized by an integer l , which correspond to spherical harmonics (SH) functions Y_l^m . These functions imbue feature vectors with rotational information, ensuring the model’s equivariance to rotations and enabling consistent geometric property analysis. This approach is key to the model’s ability to accurately represent and predict molecular and other rotationally invariant systems.

Tensor product To boost the model’s expressive power, we consider interactions between irrep features of different angular momenta l through the tensor product, which merges two irreps l_1 and l_2 into a new irrep with angular momentum l_3 . This is achieved using Clebsch-Gordan coefficients in

an expansion weighted by w_{m_1, m_2} .

$$\begin{aligned} f_{m_3}^{l_3} &= (f_{m_1}^{l_1} \otimes f_{m_2}^{l_2})_{m_3} \\ &= \sum_{m_1, m_2} w_{m_1, m_2} C_{l_1, m_1, l_2, m_2}^{l_3, m_3} f_{m_1}^{l_1} f_{m_2}^{l_2}. \end{aligned} \quad (21)$$

To reduce complexity, a depth-wise tensor product \otimes^{DTP} is adopted from the Equiformer [26, 27], utilizing internal weights to streamline computations. Input-dependent tensor product weights are denoted as \otimes_w^{DTP} , ensuring computational efficiency while preserving equivariance for feature interactions.

Table 4: A comparison of Mean Absolute Errors (MAEs) across various benchmarked models. SE3Set is trained on the MD17 dataset with a configuration of 950 training samples and 50 validation samples. Bolding shows the best model and underlining shows the second best model and the underlining tilde shows third best model. The MAEs reflect the precision of energy predictions in units of kcal/mol and forces in units of kcal/(mol·Å).

		SCHNET	DIMENET	PAINN	ET	GEMNET	NEQUIP ($l=3$)	VISNET	QUINNET	EQUIFORMER	SE3SET
ASPIRIN	ENERGY	0.37	0.204	0.167	0.123	-	0.131	0.116	<u>0.119</u>	<u>0.122</u>	0.130
	FORCE	1.35	0.499	0.338	0.253	0.217	0.184	0.155	0.145	<u>0.152</u>	<u>0.153</u>
ETHANOL	ENERGY	0.08	0.064	0.064	0.052	-	<u>0.051</u>	<u>0.051</u>	0.050	<u>0.051</u>	0.054
	FORCE	0.39	0.230	0.224	0.109	0.085	0.071	0.060	0.060	0.067	<u>0.062</u>
MALONALDEHYDE	ENERGY	0.13	0.104	0.091	0.077	-	0.076	<u>0.075</u>	0.078	0.074	0.074
	FORCE	0.66	0.383	0.319	0.169	0.155	0.129	<u>0.100</u>	0.097	0.125	<u>0.103</u>
NAPHTHALENE	ENERGY	0.16	0.122	0.116	0.085	-	0.113	0.085	<u>0.101</u>	0.085	0.113
	FORCE	0.58	0.215	0.077	0.061	0.051	0.039	0.039	0.039	0.046	0.039
SALICYLIC ACID	ENERGY	0.20	0.134	0.116	0.093	-	0.106	0.092	0.101	<u>0.099</u>	0.108
	FORCE	0.85	0.374	0.195	0.129	0.125	<u>0.090</u>	<u>0.084</u>	0.080	<u>0.090</u>	<u>0.090</u>
TOLUENE	ENERGY	0.12	0.102	0.095	0.074	-	0.092	0.074	<u>0.080</u>	<u>0.085</u>	0.093
	FORCE	0.57	0.216	0.094	0.067	0.060	<u>0.046</u>	0.039	0.039	0.048	<u>0.046</u>
URACIL	ENERGY	0.14	0.115	0.106	<u>0.095</u>	-	0.104	0.095	<u>0.096</u>	0.099	0.103
	FORCE	0.56	0.301	0.139	0.095	0.097	0.076	0.062	0.062	0.076	<u>0.067</u>

F Results of MD17

The MD17 dataset [57] features a wide variety of molecular configurations simulated at 500 K, with high-resolution trajectories and labeled with energies and forces from the PBE+vdW-TS method [60, 61]. SE3Set’s performance on this dataset is shown in Table 4. SE3Set outperforms Equiformer in accuracy, highlighting its refined force calculation capabilities. In small molecular systems, higher-order many-body interactions are less pronounced, and as a result, SE3Set does not significantly outperform other state-of-the-art (SOTA) models.

G Training details

This section outlines the training specifics, encompassing the fragmentation parameters, SE3Set hyperparameters, and certain implementation nuances utilized in our experimental setup.

Our dataset construction is founded on PyTorch Geometric [68] augmented with our fragmentation process (Sec. 4.1). Due to inconsistencies in molecular topology identified through RDKit’s sanitization routine [63], 1,403 data points were excised from the original dataset. We designated 110,000 data points for the training set and 10,000 for the validation set, selected at random.

We used an explicit overlap scheme on the QM9 and MD17 datasets because of their relatively small molecular systems. We implemented two distinct schemes for calculating fragment bond orders, following either Eq. 18 or Eq. 19. The parameters for fragmentation are detailed below. Given that the MD17 molecules are relatively small, the merge step in the fragmentation process was not actually utilized. However, we present the fragmentation parameters here for the sake of completeness.

Besides, we adopt an implicit overlap scheme on the MD22 dataset to reduce computational resource consumption. The details of cutoff r_c introduced in 4* can be found in Table 6.

On QM9 and MD17 dataset, our model was trained using a single Tesla V100 GPU with 32GB of memory, except for the 6-layer model employing the exponential bond order on QM9 dataset, which was trained on two Tesla V100 GPUs with 32GB each. For MD22 dataset, our model was trained on a single Tesla A100 GPU with 80GB of memory.

We selected $l = 2$ for our irreducible representations (irreps) feature, which includes both node and hypergraph features. For the radial basis function (RBF), we utilized Gaussian basis functions or Bessel basis functions for the QM9 dataset [55, 56] and exponential basis functions for the MD17 dataset and MD22 dataset [57]. Details could be found in Table 5 and Table 7.

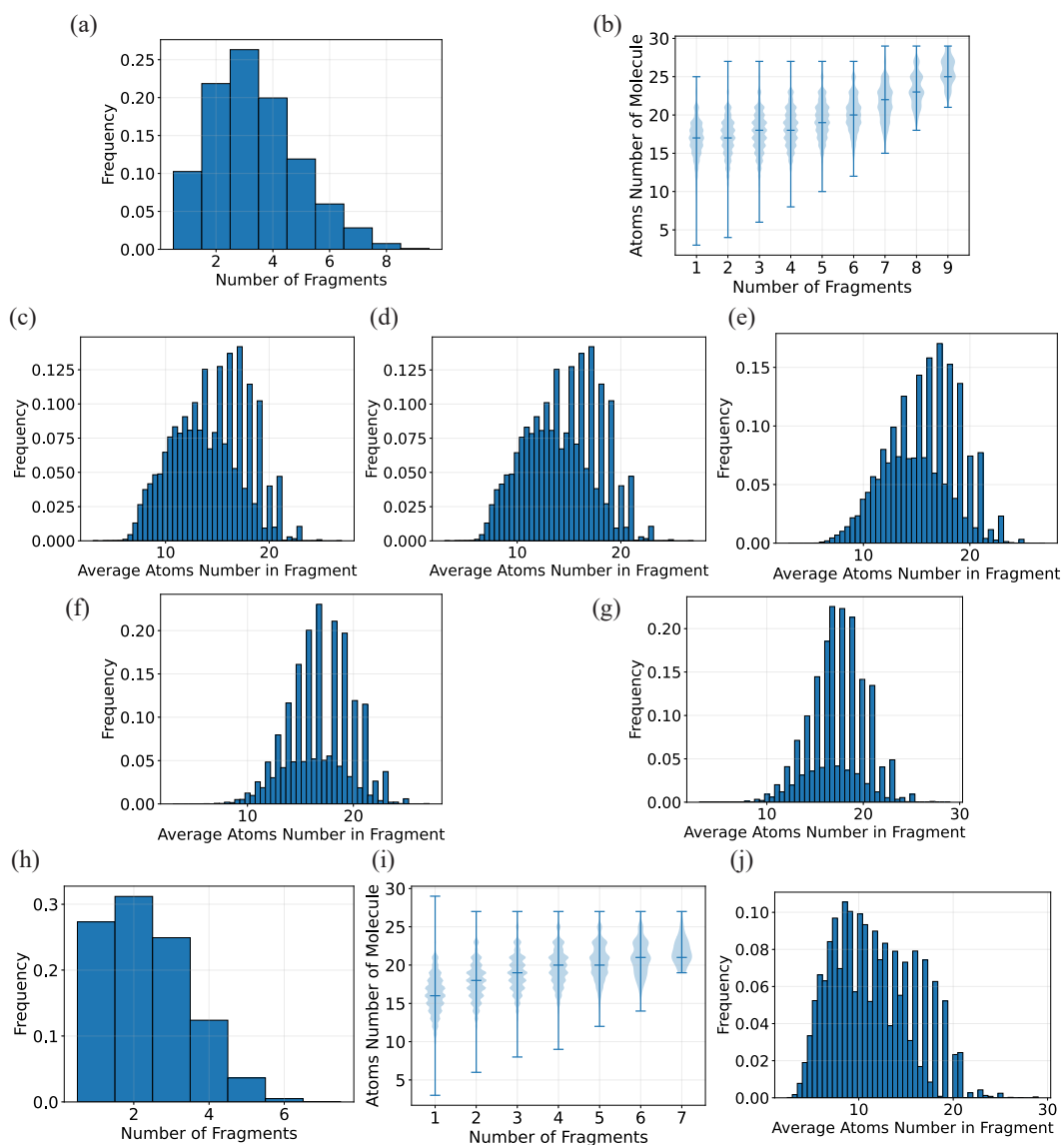


Figure 4: Distribution of fragments in QM9 dataset. (a) Fragment Count Distribution. The distribution remains consistent regardless of the value of c_w or the bond order calculation method employed. (b) Molecule Size vs. Fragment Count Distribution. Generally, the more atoms molecule has, the more fragments will generate. It is also invariant for c_w or bond order calculation scheme. Average Atom Count per Fragment Distribution (c) $c_w = 0.1$, (d) $c_w = 0.05$, (e) $c_w = 0.01$ for Lendvay bond order and (f) $c_w = 0.4$ and (g) $c_w = 0.2$ for exponential bond order, respectively. (h) BRICS Fragment Count Distribution. (i) BRICS Molecule Size vs. Fragment Count Distribution (j) BRICS Average Atom Count per Fragment.

Table 5: Hyper-parameters for fragmentation. The expand threshold does not work for models training on MD22 dataset because they adapt implicit overlap scheme.

BOND ORDER METHODS	BOND ORDER BY LENDVAY (18)	FRAGMENTATION BY EXPONENTIAL (19)
MINIMUM ATOMS NUMBER n_{\min}	2	2
MAXIMUM ATOMS NUMBER n_{\max}	6	6
ISOLATED THRESHOLD (c_{is})	0.1	0.4
EXPAND THRESHOLD (c_w)	0.1	0.2, 0.4

Table 6: Hyper-parameters for step 4* of implicit overlap scheme in MD22 experiments.

MOLECULES	AC-ALA3-NHME	DHA	STACHYOSE	AT-AT	AT-AT-CG-CG
DISTANCE CUTOFF r_c (Å)	5.0	4.0	4.0	6.0	6.0

Table 7: Hyper-parameters for training SE3Set model. In the context of hyperparameter settings for dimensions, the symbols e and o are used to denote even and odd parity, respectively.

HYPER-PARAMETERS	QM9	MD17	MD22
	VALUE OR DISCRIPTIONS	VALUE OR DISCRIPTIONS	VALUE OR DISCRIPTIONS
OPTIMIZER n_{\min}	ADAMW	ADAMW	ADAMW
LEARNING RATE SCHEDULER	COSINE	COSINE	COSINE
WARM UP EPOCHS n_{\max}	5	10	10
MINIMUM LEARNING RATE	1.0×10^{-6}	1.0×10^{-6}	1.0×10^{-6}
BATCH SIZE	32, 128	8	8
NUMBER OF EPOCHS	400	1500	1500
WEIGHT DECAY	5.0×10^{-3}	1.0×10^{-6}	1.0×10^{-6}
DROPOUT RATE	0.1	0.0	0.0
RBF CUTOFF (Å)	42.0	MAX DISTANCE OF USED ATOM PAIRS	
NUMBER OF BASIS	128(GAUSSIAN), 8(BESSEL)	32(EXPONENTIAL)	32(EXPONENTIAL)
NUMBER OF BLOCKS	3, 6	3, 6	6
NODE EMBEDDING DIMENSION		[(128, 0e), (64, 1o), (32, 2e)]	
HYPEREDGE EMBEDDING DIMENSION		[(128, 0e), (64, 1o), (32, 2e)]	
ATTENTION HEAD DIMENSION		[(32, 0e), (16, 1o), (8, 2e)]	
FEED FORWARD DIMENSION		[(384, 0e), (192, 1o), (96, 2e)]	
OUTPUT FEATURE DIMENSION		[(512, 0e)]	

NeurIPS Paper Checklist

1. Claims

Question: Do the main claims made in the abstract and introduction accurately reflect the paper's contributions and scope?

Answer: [Yes]

Justification: The abstract and introduction have clearly stated the claims made, including the contributions made in the paper. The related material for the question can be found in abstract section.

Guidelines:

- The answer NA means that the abstract and introduction do not include the claims made in the paper.
- The abstract and/or introduction should clearly state the claims made, including the contributions made in the paper and important assumptions and limitations. A No or NA answer to this question will not be perceived well by the reviewers.
- The claims made should match theoretical and experimental results, and reflect how much the results can be expected to generalize to other settings.
- It is fine to include aspirational goals as motivation as long as it is clear that these goals are not attained by the paper.

2. Limitations

Question: Does the paper discuss the limitations of the work performed by the authors?

Answer: [Yes]

Justification: The related material for the question can be found in Sec. 4.1 and Sec. 5.2.

Guidelines:

- The answer NA means that the paper has no limitation while the answer No means that the paper has limitations, but those are not discussed in the paper.
- The authors are encouraged to create a separate "Limitations" section in their paper.
- The paper should point out any strong assumptions and how robust the results are to violations of these assumptions (e.g., independence assumptions, noiseless settings, model well-specification, asymptotic approximations only holding locally). The authors should reflect on how these assumptions might be violated in practice and what the implications would be.
- The authors should reflect on the scope of the claims made, e.g., if the approach was only tested on a few datasets or with a few runs. In general, empirical results often depend on implicit assumptions, which should be articulated.
- The authors should reflect on the factors that influence the performance of the approach. For example, a facial recognition algorithm may perform poorly when image resolution is low or images are taken in low lighting. Or a speech-to-text system might not be used reliably to provide closed captions for online lectures because it fails to handle technical jargon.
- The authors should discuss the computational efficiency of the proposed algorithms and how they scale with dataset size.
- If applicable, the authors should discuss possible limitations of their approach to address problems of privacy and fairness.
- While the authors might fear that complete honesty about limitations might be used by reviewers as grounds for rejection, a worse outcome might be that reviewers discover limitations that aren't acknowledged in the paper. The authors should use their best judgment and recognize that individual actions in favor of transparency play an important role in developing norms that preserve the integrity of the community. Reviewers will be specifically instructed to not penalize honesty concerning limitations.

3. Theory Assumptions and Proofs

Question: For each theoretical result, does the paper provide the full set of assumptions and a complete (and correct) proof?

Answer: [Yes]

Justification: The related material for the question can be found in Sec. 4.1 and Appendix.

Guidelines:

- The answer NA means that the paper does not include theoretical results.
- All the theorems, formulas, and proofs in the paper should be numbered and cross-referenced.
- All assumptions should be clearly stated or referenced in the statement of any theorems.
- The proofs can either appear in the main paper or the supplemental material, but if they appear in the supplemental material, the authors are encouraged to provide a short proof sketch to provide intuition.
- Inversely, any informal proof provided in the core of the paper should be complemented by formal proofs provided in appendix or supplemental material.
- Theorems and Lemmas that the proof relies upon should be properly referenced.

4. Experimental Result Reproducibility

Question: Does the paper fully disclose all the information needed to reproduce the main experimental results of the paper to the extent that it affects the main claims and/or conclusions of the paper (regardless of whether the code and data are provided or not)?

Answer: [Yes]

Justification: We have provided all the information needed to reproduce experimental results in Appendix G. The code will be open source after the paper is accepted.

Guidelines:

- The answer NA means that the paper does not include experiments.
- If the paper includes experiments, a No answer to this question will not be perceived well by the reviewers: Making the paper reproducible is important, regardless of whether the code and data are provided or not.
- If the contribution is a dataset and/or model, the authors should describe the steps taken to make their results reproducible or verifiable.
- Depending on the contribution, reproducibility can be accomplished in various ways. For example, if the contribution is a novel architecture, describing the architecture fully might suffice, or if the contribution is a specific model and empirical evaluation, it may be necessary to either make it possible for others to replicate the model with the same dataset, or provide access to the model. In general, releasing code and data is often one good way to accomplish this, but reproducibility can also be provided via detailed instructions for how to replicate the results, access to a hosted model (e.g., in the case of a large language model), releasing of a model checkpoint, or other means that are appropriate to the research performed.
- While NeurIPS does not require releasing code, the conference does require all submissions to provide some reasonable avenue for reproducibility, which may depend on the nature of the contribution. For example
 - (a) If the contribution is primarily a new algorithm, the paper should make it clear how to reproduce that algorithm.
 - (b) If the contribution is primarily a new model architecture, the paper should describe the architecture clearly and fully.
 - (c) If the contribution is a new model (e.g., a large language model), then there should either be a way to access this model for reproducing the results or a way to reproduce the model (e.g., with an open-source dataset or instructions for how to construct the dataset).
 - (d) We recognize that reproducibility may be tricky in some cases, in which case authors are welcome to describe the particular way they provide for reproducibility. In the case of closed-source models, it may be that access to the model is limited in some way (e.g., to registered users), but it should be possible for other researchers to have some path to reproducing or verifying the results.

5. Open access to data and code

Question: Does the paper provide open access to the data and code, with sufficient instructions to faithfully reproduce the main experimental results, as described in supplemental material?

Answer: [Yes]

Justification: The code will be open source after the paper is accepted.

Guidelines:

- The answer NA means that paper does not include experiments requiring code.
- Please see the NeurIPS code and data submission guidelines (<https://nips.cc/public/guides/CodeSubmissionPolicy>) for more details.
- While we encourage the release of code and data, we understand that this might not be possible, so “No” is an acceptable answer. Papers cannot be rejected simply for not including code, unless this is central to the contribution (e.g., for a new open-source benchmark).
- The instructions should contain the exact command and environment needed to run to reproduce the results. See the NeurIPS code and data submission guidelines (<https://nips.cc/public/guides/CodeSubmissionPolicy>) for more details.
- The authors should provide instructions on data access and preparation, including how to access the raw data, preprocessed data, intermediate data, and generated data, etc.
- The authors should provide scripts to reproduce all experimental results for the new proposed method and baselines. If only a subset of experiments are reproducible, they should state which ones are omitted from the script and why.
- At submission time, to preserve anonymity, the authors should release anonymized versions (if applicable).
- Providing as much information as possible in supplemental material (appended to the paper) is recommended, but including URLs to data and code is permitted.

6. Experimental Setting/Details

Question: Does the paper specify all the training and test details (e.g., data splits, hyperparameters, how they were chosen, type of optimizer, etc.) necessary to understand the results?

Answer: [Yes]

Justification: We have provided all the information needed to reproduce experimental results in Appendix G.

Guidelines:

- The answer NA means that the paper does not include experiments.
- The experimental setting should be presented in the core of the paper to a level of detail that is necessary to appreciate the results and make sense of them.
- The full details can be provided either with the code, in appendix, or as supplemental material.

7. Experiment Statistical Significance

Question: Does the paper report error bars suitably and correctly defined or other appropriate information about the statistical significance of the experiments?

Answer: [Yes]

Justification: The mean and variance of the experimental results are reported in Fig. 4.

Guidelines:

- The answer NA means that the paper does not include experiments.
- The authors should answer "Yes" if the results are accompanied by error bars, confidence intervals, or statistical significance tests, at least for the experiments that support the main claims of the paper.
- The factors of variability that the error bars are capturing should be clearly stated (for example, train/test split, initialization, random drawing of some parameter, or overall run with given experimental conditions).

- The method for calculating the error bars should be explained (closed form formula, call to a library function, bootstrap, etc.)
- The assumptions made should be given (e.g., Normally distributed errors).
- It should be clear whether the error bar is the standard deviation or the standard error of the mean.
- It is OK to report 1-sigma error bars, but one should state it. The authors should preferably report a 2-sigma error bar than state that they have a 96% CI, if the hypothesis of Normality of errors is not verified.
- For asymmetric distributions, the authors should be careful not to show in tables or figures symmetric error bars that would yield results that are out of range (e.g. negative error rates).
- If error bars are reported in tables or plots, The authors should explain in the text how they were calculated and reference the corresponding figures or tables in the text.

8. Experiments Compute Resources

Question: For each experiment, does the paper provide sufficient information on the computer resources (type of compute workers, memory, time of execution) needed to reproduce the experiments?

Answer: [Yes]

Justification: We have provided all the information in Appendix G.

Guidelines:

- The answer NA means that the paper does not include experiments.
- The paper should indicate the type of compute workers CPU or GPU, internal cluster, or cloud provider, including relevant memory and storage.
- The paper should provide the amount of compute required for each of the individual experimental runs as well as estimate the total compute.
- The paper should disclose whether the full research project required more compute than the experiments reported in the paper (e.g., preliminary or failed experiments that didn't make it into the paper).

9. Code Of Ethics

Question: Does the research conducted in the paper conform, in every respect, with the NeurIPS Code of Ethics <https://neurips.cc/public/EthicsGuidelines?>

Answer:[Yes]

Justification: We have reviewed the NeurIPS Code of Ethics.

Guidelines:

- The answer NA means that the authors have not reviewed the NeurIPS Code of Ethics.
- If the authors answer No, they should explain the special circumstances that require a deviation from the Code of Ethics.
- The authors should make sure to preserve anonymity (e.g., if there is a special consideration due to laws or regulations in their jurisdiction).

10. Broader Impacts

Question: Does the paper discuss both potential positive societal impacts and negative societal impacts of the work performed?

Answer: [NA]

Justification: There is no societal impact of the work performed.

Guidelines:

- The answer NA means that there is no societal impact of the work performed.
- If the authors answer NA or No, they should explain why their work has no societal impact or why the paper does not address societal impact.
- Examples of negative societal impacts include potential malicious or unintended uses (e.g., disinformation, generating fake profiles, surveillance), fairness considerations (e.g., deployment of technologies that could make decisions that unfairly impact specific groups), privacy considerations, and security considerations.

- The conference expects that many papers will be foundational research and not tied to particular applications, let alone deployments. However, if there is a direct path to any negative applications, the authors should point it out. For example, it is legitimate to point out that an improvement in the quality of generative models could be used to generate deepfakes for disinformation. On the other hand, it is not needed to point out that a generic algorithm for optimizing neural networks could enable people to train models that generate Deepfakes faster.
- The authors should consider possible harms that could arise when the technology is being used as intended and functioning correctly, harms that could arise when the technology is being used as intended but gives incorrect results, and harms following from (intentional or unintentional) misuse of the technology.
- If there are negative societal impacts, the authors could also discuss possible mitigation strategies (e.g., gated release of models, providing defenses in addition to attacks, mechanisms for monitoring misuse, mechanisms to monitor how a system learns from feedback over time, improving the efficiency and accessibility of ML).

11. Safeguards

Question: Does the paper describe safeguards that have been put in place for responsible release of data or models that have a high risk for misuse (e.g., pretrained language models, image generators, or scraped datasets)?

Answer: [NA]

Justification: The paper poses no such risks.

Guidelines:

- The answer NA means that the paper poses no such risks.
- Released models that have a high risk for misuse or dual-use should be released with necessary safeguards to allow for controlled use of the model, for example by requiring that users adhere to usage guidelines or restrictions to access the model or implementing safety filters.
- Datasets that have been scraped from the Internet could pose safety risks. The authors should describe how they avoided releasing unsafe images.
- We recognize that providing effective safeguards is challenging, and many papers do not require this, but we encourage authors to take this into account and make a best faith effort.

12. Licenses for existing assets

Question: Are the creators or original owners of assets (e.g., code, data, models), used in the paper, properly credited and are the license and terms of use explicitly mentioned and properly respected?

Answer: [Yes]

Justification: All the data can be found publicly, and the code will be open source after the paper is accepted.

Guidelines:

- The answer NA means that the paper does not use existing assets.
- The authors should cite the original paper that produced the code package or dataset.
- The authors should state which version of the asset is used and, if possible, include a URL.
- The name of the license (e.g., CC-BY 4.0) should be included for each asset.
- For scraped data from a particular source (e.g., website), the copyright and terms of service of that source should be provided.
- If assets are released, the license, copyright information, and terms of use in the package should be provided. For popular datasets, paperswithcode.com/datasets has curated licenses for some datasets. Their licensing guide can help determine the license of a dataset.
- For existing datasets that are re-packaged, both the original license and the license of the derived asset (if it has changed) should be provided.

- If this information is not available online, the authors are encouraged to reach out to the asset’s creators.

13. **New Assets**

Question: Are new assets introduced in the paper well documented and is the documentation provided alongside the assets?

Answer: [NA]

Justification: The paper does not release new assets.

Guidelines:

- The answer NA means that the paper does not release new assets.
- Researchers should communicate the details of the dataset/code/model as part of their submissions via structured templates. This includes details about training, license, limitations, etc.
- The paper should discuss whether and how consent was obtained from people whose asset is used.
- At submission time, remember to anonymize your assets (if applicable). You can either create an anonymized URL or include an anonymized zip file.

14. **Crowdsourcing and Research with Human Subjects**

Question: For crowdsourcing experiments and research with human subjects, does the paper include the full text of instructions given to participants and screenshots, if applicable, as well as details about compensation (if any)?

Answer: [NA]

Justification: The paper does not involve crowdsourcing nor research with human subjects.

Guidelines:

- The answer NA means that the paper does not involve crowdsourcing nor research with human subjects.
- Including this information in the supplemental material is fine, but if the main contribution of the paper involves human subjects, then as much detail as possible should be included in the main paper.
- According to the NeurIPS Code of Ethics, workers involved in data collection, curation, or other labor should be paid at least the minimum wage in the country of the data collector.

15. **Institutional Review Board (IRB) Approvals or Equivalent for Research with Human Subjects**

Question: Does the paper describe potential risks incurred by study participants, whether such risks were disclosed to the subjects, and whether Institutional Review Board (IRB) approvals (or an equivalent approval/review based on the requirements of your country or institution) were obtained?

Answer: [NA]

Justification: The paper does not involve crowdsourcing nor research with human subjects.

Guidelines:

- The answer NA means that the paper does not involve crowdsourcing nor research with human subjects.
- Depending on the country in which research is conducted, IRB approval (or equivalent) may be required for any human subjects research. If you obtained IRB approval, you should clearly state this in the paper.
- We recognize that the procedures for this may vary significantly between institutions and locations, and we expect authors to adhere to the NeurIPS Code of Ethics and the guidelines for their institution.
- For initial submissions, do not include any information that would break anonymity (if applicable), such as the institution conducting the review.